Acta Crystallographica Section C
Crystal Structure Communications
ISSN 0108-2701

The tunnel manganese oxide $Na_{4.32}Mn_9O_{18}$: a new Na^+ site discovered by single-crystal X-ray diffraction

Qingxin Chu, Xiaofeng Wang, Qiliang Li and Xiaoyang Liu*

State Key Laboratory of Inorganic Synthesis and Preparative Chemistry, Jilin University, Changchun 130012, People's Republic of China
Correspondence e-mail: liuxy@jlu.edu.cn

Received 25 October 2010
Accepted 16 December 2010
Online 7 January 2011

The title compound, tetrasodium nonamanganese octadecaoxide, $Na_{4.32}Mn_9O_{18}$, was synthesized by reacting Mn_2O_3 with NaCl. One Mn atom occupies a site of 2/*m* symmetry, while all other atoms sit on mirror planes. The compound is isostructural with $Na_4Ti_4Mn_5O_{18}$ and suggestive of Mn^{3+}/Mn^{4+} charge ordering. It has a double-tunnel structure built up from double and triple chains of MnO_6 octahedra and single chains of MnO_5 square pyramids by corner sharing. Disordered Na^+ cations occupy four crystallographic sites within the tunnels, including an unexpected new Na^+ site discovered inside the large S-shaped tunnel. A local-ordering model is used to show the possible Na^+ distribution, and the unit-cell evolution during charging/discharging is explained on the basis of this local-ordering model.

Comment

$Na_4Mn_9O_{18}$ has been investigated as an electrode material (Hosono *et al.*, 2008; Sauvage, Laffont *et al.*, 2007) and a sodium-ion sensor (Sauvage, Baudrin *et al.*, 2007) because of its unique double-tunnel structure which can facilitate Na^+ mobility. The crystal structure of $Na_4Mn_9O_{18}$ was believed to be essentially similar to that of $Na_4Mn_4Ti_5O_{18}$ (Mumme, 1968; Parant *et al.*, 1971), and this has been verified by Rietveld refinement against powder X-ray (Floros *et al.*, 2001; Doeff *et al.*, 1996) and neutron (Armstrong *et al.*, 1998) diffraction data. To date, however, the small crystal size of $Na_4Mn_9O_{18}$ samples has prevented accurate structure refinement from single-crystal data. In previous reports, there were some indications that the sodium stoichiometry in $Na_4Mn_9O_{18}$ was higher than 4 (Jeong & Manthiram, 2001), suggesting a more complicated distribution of Na^+ ions in the tunnels compared with that established to date.

We report here the structure of the title compound, $Na_{4.32}Mn_9O_{18}$, which was prepared by reacting Mn_2O_3 with NaCl. $Na_{4.32}Mn_9O_{18}$ crystallizes in an orthorhombic structure (space group *Pbam*) that contains 18 crystallographically independent atoms, *viz.* five Mn, nine O and four Na. The refined framework structure is consistent with the structure model of $Na_4Mn_4Ti_5O_{18}$ (Mumme, 1968). Specifically, the $Na_{4.32}Mn_9O_{18}$ crystal structure is composed of single chains of edge-linked MnO_5 square pyramids (Mn3) and double (Mn1 and Mn5) and triple (Mn2 and two Mn4) chains of edge-linked MnO_6 octahedra. Each central MnO_6 octahedron of the triple chains (Mn2) shares six edges with six neighbouring distorted octahedra. These single, double and triple chains share the vertices of the polyhedra and form two types of tunnel parallel to the *c* axis, namely large S-shaped tunnels and small six-sided tunnels (Figs. 1 and 2). The large tunnel comprises ten MnO_6 octahedra and two MnO_5 square pyramids, while the small tunnel is composed of four MnO_6 octahedra and two MnO_5 square pyramids.

A tendency for Mn^{3+}/Mn^{4+} charge ordering within $Na_{1.1}Ca_{1.8}Mn_9O_{18}$ has been proposed, based on both the insulating

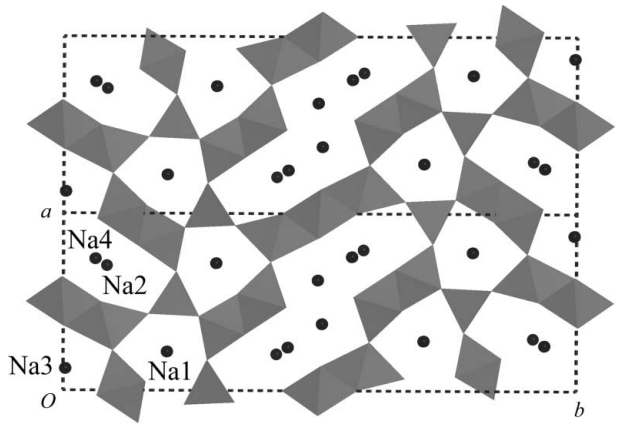

Figure 1
A polyhedral representation of the crystal structure of $Na_{4.32}Mn_9O_{18}$, viewed down the *c* axis. The Na sites in the asymmetric unit are labelled.

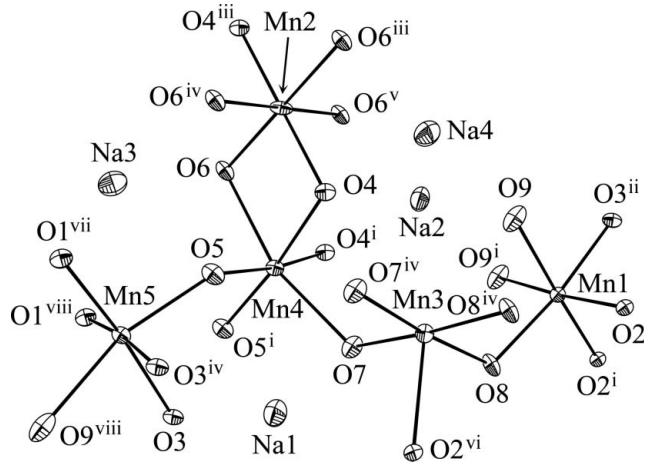

Figure 2
The coordination environment of the Mn atoms in the title compound. Displacement ellipsoids are drawn at the 50% probability level. [Symmetry codes: (i) $x, y, z+1$; (ii) $x+1, y, z$; (iii) $-x+1, -y, -z$; (iv) $x, y, z-1$; (v) $-x+1, -y, -z+1$; (vi) $x-\frac{1}{2}, -y+\frac{1}{2}, z$; (vii) $x-1, y, z-1$; (viii) $x-1, y, z$.]

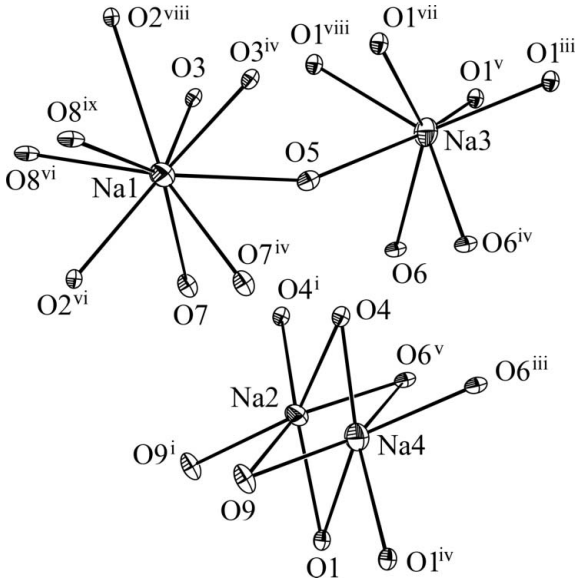

Figure 3
The coordination environment of the Na atoms in the title compound. Displacement ellipsoids are drawn at the 50% probability level. [Symmetry codes are as listed in Fig 1; additionally: (ix) $x - \frac{1}{2}, -y + \frac{1}{2}, z - 1$.]

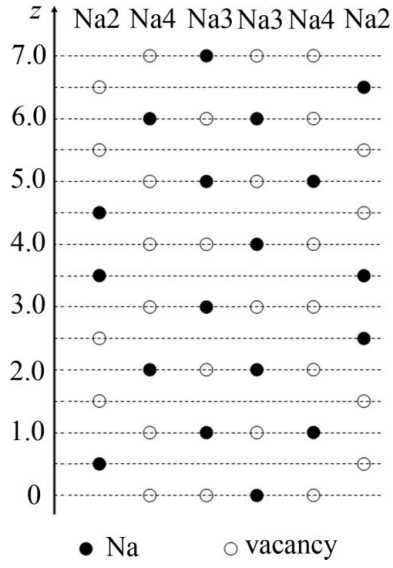

Figure 4
The possible ordered Na^+ arrangement within the S-shaped tunnel.

nature of the compound and the Mn—O bond lengths refined from powder X-ray diffraction data (Floros *et al.*, 2001). In $Na_{4.32}Mn_9O_{18}$, Mn^{3+} is likely to occupy preferentially the Mn3 and Mn4 sites, since these have relatively elongated environments (Table 1). Hence, charge ordering of Mn^{3+}/Mn^{4+} is also suggested by the structure of $Na_{4.32}Mn_9O_{18}$.

Four crystallographically distinct Na^+ sites exist within the tunnels of $Na_{4.32}Mn_9O_{18}$. Na1 resides in the six-sided tunnel, while the others (Na2, Na3 and Na4) reside in the large S-shaped tunnel (Fig. 1). The Na^+ sites are all positioned on mirror planes perpendicular to the *c* axis. Na1 is coordinated by nine O atoms (Fig. 3). The O3, O7 and O8 sites on each side of the mirror plane form a triangular prism, while three additional O atoms on the mirror plane are located out from the three prism faces. The coordination polyhedra of atoms Na2, Na3 and Na4 are essentially similar to that of Na1 (Fig. 3). In each case, the Na atom is again at the centre of a triangular prism, while Na3 has an additional O atom out from a face. Atoms Na1, Na3 and Na4 are located at $z = 0$, while atom Na2 is located at $z = \frac{1}{2}$. Na4 resides between Na2 and Na3, where the nearest Na4—Na2 and Na4—Na3 distances are 1.569 (5) and 2.125 (11) Å, respectively. This excludes simultaneous occupation of the Na4 site and neighbouring Na2 or Na3 sites, and suggests that the occupancy of the Na4 site is low. The Na1 site located in the six-sided tunnel has a refined occupancy of 0.922 (9), while the Na sites (Na2, Na3 and Na4) in the S-shaped tunnel have refined occupancies of 0.474 (9), 0.532 (9) and 0.233 (9), respectively. The sample composition refines overall to be $Na_{4.32}Mn_9O_{18}$, in good agreement with energy-dispersive spectroscopy results, which show an Na:Mn ratio of 1:2.

The Na stoichiometry in $Na_4Mn_9O_{18}$ has previously been recognized to be higher than 4 (Jeong & Manthiram, 2001), although the reason for this has remained unclear. The Na4 site discovered here accounts for the excess Na^+ within the structure. The Na4 site may be attributable to the repulsion balance of Na^+ within the tunnel. Because the Na2, Na3 and Na4 sites are not fully occupied, coupled with the fact that there is no evidence from the single-crystal or powder X-ray diffraction data to indicate long-range ordering of Na^+, the Na^+ ions are likely situated with a short-range order within each tunnel (Armstrong *et al.*, 1998). The scheme of the ordering will rely on the distances between the Na2, Na3 and Na4 sites in the S-shaped tunnel. In general, the Na^+ ions should be distributed evenly on the sites within the S-shaped tunnel to achieve repulsion balance. It is noteworthy that Na3 and Na4 have the same *z* value, but they are not likely to appear in the same cell with the same *z* value.

Fig. 4 shows a possible local ordered distribution of Na^+ in the S-shaped tunnel. Because of the existence of the additional Na4 site, the ordering scheme is more complicated than that proposed by Armstrong *et al.* (1998). The nearest distance between Na2 and Na4 [1.569 (5) Å] is avoided. The repulsions between Na2 and Na3, Na4 and Na3, and Na2 and Na4 are all balanced. Finally, the resulting occupancies of Na2, Na3 and Na4 are $\frac{1}{2}$, $\frac{1}{2}$ and $\frac{1}{4}$, respectively, corresponding to an ideal composition of $Na_{4.5}Mn_9O_{18}$ (equivalent to $Na_{0.5}MnO_2$).

It has been reported that the unit cell of $Na_4Mn_9O_{18}$ varies with Na content upon charging/discharging, in which only the Na2 and Na3 sites in the S-shaped tunnel are movable (Sauvage, Baudrin *et al.*, 2007). Sodium deinsertion from $Na_4Mn_9O_{18}$ results in a decrease in *b* (with *a* and *c* remaining essentially unchanged), while sodium insertion causes slight variation of *b* with a large variation of *a* and *c*. The existence of the Na4 site between Na2 and Na3 results in fewer vacant sites and stronger repulsion along *b* than along *a* and *c*, which may make the lattice strain along *b* reach its upper limit at the composition $Na_{4.5}Mn_9O_{18}$. As a result, sodium deinsertion from $Na_{4.5}Mn_9O_{18}$, no matter from which site in the S-shaped

tunnel, relieves the lattice strain along *b* and leads to a larger contraction along *b* than along *a* and *c*. In contrast, sodium insertion into $Na_{4.5}Mn_9O_{18}$ will mainly diffuse into the Na2 and Na3 sites, because the nearest distance between Na2 and Na4 is too small for Na4 to be accessed. Therefore, the vacancy along *a* and *c* is preferentially filled, which leads to expansion mainly along *a* and *c*.

Experimental

NaCl (AR grade) was supplied by Beijing Chemical Reagent Company, China. Mn_2O_3 (99%) was purchased from Aldrich. In a typical synthesis, Mn_2O_3 and NaCl were mixed together in a 1:20 molar ratio. The mixture was ground in an agate mortar, then transferred to an alumina crucible and kept at 1123 K for 12 h in a muffle furnace. When the reaction was complete, the product was allowed to cool naturally to room temperature in the muffle furnace, then it was collected, mixed with an appropriate amount of distilled water and sonicated for 10 min. The crude product was finally rinsed with distilled water five times to remove NaCl, before being dried in an oven at 333 K overnight to give the final product. Elemental analysis was performed by energy-dispersive spectroscopy (EDS) using an Oxford INCA energy-dispersive analyser. The result shows an Na:Mn ratio of 0.5.

Crystal data

$Na_{4.32}Mn_9O_{18}$
M_r = 881.78
Orthorhombic, *Pbam*
a = 9.084 (4) Å
b = 26.311 (10) Å
c = 2.8223 (11) Å
V = 674.6 (5) Å^3
Z = 2
Mo *K*α radiation
μ = 8.38 mm^{-1}
T = 296 K
0.3 × 0.01 × 0.01 mm

Data collection

Bruker SMART APEXII CCD diffractometer
Absorption correction: multi-scan (*SADABS*; Bruker, 2009)
T_{min} = 0.656, T_{max} = 0.746
4301 measured reflections
1099 independent reflections
912 reflections with $I > 2\sigma(I)$
R_{int} = 0.035

Refinement

$R[F^2 > 2\sigma(F^2)]$ = 0.032
$wR(F^2)$ = 0.068
S = 1.09
1099 reflections
111 parameters
Δρ$_{max}$ = 0.94 e Å^{-3}
Δρ$_{min}$ = −0.72 e Å^{-3}

Mn and O atoms could be located unambiguously. Atoms Na1, Na2 and Na3 were subsequently located from a difference Fourier map and their site-occupancy factors were refined. At the end of this refinement, *R*1 reached 0.059 and all atom sites of the analogous $Na_4Mn_4Ti_5O_{18}$ structure (Mumme, 1968) were accounted for. At this stage, a peak of about 4 e Å^{-3} remained in the residual electron density within the S-shaped tunnel, which was included as atom Na4. Subsequent refinement including the site-occupancy factor of Na4 provided the final structure, with *R*1 = 0.044.

Table 1
Selected bond lengths (Å).

Mn1—O2	1.866 (2)	Mn4—O4	1.928 (2)
Mn1—O8	1.902 (4)	Mn4—O5	1.886 (2)
Mn1—O9	1.924 (2)	Mn4—O6	2.261 (4)
Mn2—O4	1.919 (3)	Mn4—O7	2.133 (3)
Mn2—O6	1.901 (2)	Mn5—O3	1.943 (2)
Mn3—O7	1.892 (2)	Mn5—O5	1.937 (4)
Mn3—O8	1.926 (2)	Mn5—O1^{vii}	1.869 (2)
Mn3—O2^{vi}	2.146 (3)		

Symmetry codes: (vi) $x-\frac{1}{2}, -y+\frac{1}{2}, z$; (vii) $x-1, y, z-1$.

Data collection: *APEX2* (Bruker, 2009); cell refinement: *SAINT* (Bruker, 2009); data reduction: *SAINT*; program(s) used to solve structure: *SHELXS97* (Sheldrick, 2008); program(s) used to refine structure: *SHELXL97* (Sheldrick, 2008); molecular graphics: *SHELXL97* and *Materials Studio* (Accelrys, 2005); software used to prepare material for publication: *SHELXL97* and *publCIF* (Westrip, 2010).

This work was supported by the National Natural Science Foundation of China (grant Nos. 20471022 and 40673051).

Supplementary data for this paper are available from the IUCr electronic archives (Reference: BI3006). Services for accessing these data are described at the back of the journal.

References

Accelrys (2005). *Materials Studio*. Release 3.2. Accelrys Software Inc., San Diego, California, USA.
Armstrong, A. R., Huang, H., Jennings, R. A. & Bruce, P. G. (1998). *J. Mater. Chem.* **8**, 255–259.
Bruker (2009). *APEX2*, *SAINT* and *SADABS*. Bruker AXS Inc., Madison, Wisconsin, USA.
Doeff, M. M., Richardson, T. J. & Kepley, L. (1996). *J. Electrochem. Soc.* **143**, 2507–2516.
Floros, N., Michel, C., Hervieu, M. & Raveau, B. (2001). *J. Solid State Chem.* **162**, 34–41.
Hosono, E., Matsuda, H., Honma, I., Fujihara, S., Ichihara, M. & Zhou, H. S. (2008). *J. Power Sources*, **182**, 349–352.
Jeong, Y. U. & Manthiram, A. (2001). *J. Solid State Chem.* **156**, 331–338.
Mumme, W. G. (1968). *Acta Cryst.* B**24**, 1114–1120.
Parant, J. P., Olazcuaga, R., Devalette, M., Fouassier, C. & Hagenmuller, P. (1971). *J. Solid State Chem.* **3**, 1–11.
Sauvage, F., Baudrin, E. & Tarascon, J. M. (2007). *Sens. Actuators B*, **120**, 638–644.
Sauvage, F., Laffont, L., Tarascon, J. M. & Baudrin, E. (2007). *Inorg. Chem.* **46**, 3289–3294.
Sheldrick, G. M. (2008). *Acta Cryst.* A**64**, 112–122.
Westrip, S. P. (2010). *J. Appl. Cryst.* **43**, 920–925.